PHYSICAL REVIEW B **74**, 113110 (2006)

Core-level in rare-earth metals and their trifluorides from exchange splitting photoemission and ground-state calculations

W. Burian[*] and J. Szade
A. Chełkowski Institute of Physics, University of Silesia, ul. Uniwersytecka 4, 40-007 Katowice, Poland

J. Deniszczyk
Institute of Materials Science, University of Silesia, ul. Bankowa 12, 40-007 Katowice, Poland

T. O'Keevan and Z. Celinski
Center for Magnetism and Magnetic Nanostructures, University of Colorado at Colorado Springs, 1420 Austin Bluffs Pkwy, Colorado Springs, Colorado 80918, USA

(Received 7 August 2005; revised manuscript received 7 June 2006; published 29 September 2006)

Photoemission from Eu, Gd, Tb, and their trifluorides has been investigated with respect to exchange splitting of core-levels. For EuF_3, a splitting of the 4s and 5s lines has been observed despite the nonmagnetic Eu ion ground state. The major part of the observed splittings is reproduced by the density-functional theory based calculations. This indicates that the exchange splitting of the core-levels is present in the photoemission initial state of rare-earth ions with partially filled 4f shell.

DOI: 10.1103/PhysRevB.74.113110 PACS number(s): 71.20.Eh, 79.60.−i, 71.15.Mb, 31.15.Ar

I. INTRODUCTION

The structure of photoemission multiplets in rare earths and their compounds is connected with the presence of the magnetic moment in the partially filled 4f shell and was usually explained with use of atomic models.[1] According to these models, the multiplets are formed due to the exchange interaction of a photohole with the local spin of a rare-earth 4f shell. For s core-levels, it leads to the splitting of photoemission lines, while for other levels, the complex multiplets are observed due to the additional spin-orbit interaction. Detailed studies of the multiplet structure were based mainly on the results obtained for pure Gd and its compounds.[2,3] The structure of the Eu 4s and 5s spectra has not yet been analyzed in detail. Europium metal and most Eu intermetallic compounds are divalent with the electron configuration $[Xe]4f^7 6s^2$. The ground state of the f shell is then the same as for a Gd^{3+} ion: $L=0$, $S=7/2$, $J=7/2$. Europium is trivalent in ionic and some metallic compounds and, according to the Hund's rules, the total momentum of the 4f shell is zero: $L=3$, $S=3$, $J=0$. The photoemission from EuF_3, $EuCl_3$, and Eu_2O_3 has been investigated previously, but no exchange splitting was reported.[4] For these materials, the presence of emission from Eu^{2+} has been detected in a form of low-energy satellites in the 3d and 4d spectra. These satellites can be attributed to Eu^{2+} states, which are formed at the surface.[4,5] Our recent work on EuF_3 showed that the molecular beam epitaxy (MBE) grown ultrathin layers do not exhibit surface valence transition.[5,6]

In this work, we present the analysis of the s levels splitting in elemental rare-earth (RE) metals (Eu, Gd, Tb) and their trifluorides (EuF_3, GdF_3, TbF_3). We compare the photoemission experimental data with those calculated by means of the all electron *ab initio* electronic structure methods developed for solids. Our calculations indicate that the exchange splitting of the core s levels is present in the initial state of the photoemission process. The calculated magnitudes of exchange splitting agree surprisingly well with the experimental data. A good agreement was obtained even though the calculations neglected the final-state effects.

One can conjecture that the final-state effects determine the detailed shape of the core-level photoemission spectra, including the intensity ratio of the split components. This feature is usually correctly reproduced by the atomic calculations employing the configuration interaction method.[1]

II. EXPERIMENTAL AND CALCULATIONAL DETAILS

A thin-film sample was grown on a GaAs substrate (using the MBE technique) under a pressure of 10^{-10} Torr. The MBE prepared structure consisted of Fe (0.7 nm), Ag (75 nm), Fe (4 nm), Au (5 nm), Fe (3.9 nm), and EuF_3 (0.8 nm) layers, in this order. The reflection high-energy electron diffraction clearly showed that EuF_3 grows in single-crystal form on the Fe(001) layer. The XPS measurements were performed using a PHI 5700 Photoelectron Spectrometer from Physical Electronics, using monochromatized AlK_α radiation (the energy resolution was approximately 0.35 eV). The vacuum during measurements was about 10^{-10} Torr.

The calculations of the electronic structure have been performed using the general potential linear augmented plane-wave (FP-LAPW) method, using the WIEN2k code of Blaha *et al.*[7] In the FP-LAPW approach, no shape approximation is used and the crystal potential is expanded into spherical (lattice) harmonics within the muffin-tin (MT) atomic spheres and into plane waves outside MT spheres. The electronic structure calculations for all materials were performed using the experimental lattice parameters.[8–13]

The gradient corrected local spin-density approximation (LSDA) for the exchange correlation (XC) potential was used in the form developed by Perdew, Burke, and Ernzerhof

(PBE).[14] To account for the Hubbard correlation interaction within the $4f$-band states in the electronic structure of hcp-Gd, Eu, and Tb, the FP-LAPW method was employed with the use of the PBE XC potential, corrected according to the LSDA+U method.[15] The LSDA+U XC potential was implemented for the $4f$ orbitals. Values of the Coulomb (U) and exchange (J) parameters for Gd were equal to 6.8 and 0.68 eV, respectively.[16] For Eu and Tb elements the U and J parameters were chosen in order to obtain the proper binding energy of $4f$ states (U=4.8 eV for Eu and U=6.8 eV for Tb). The number of $\vec{k}$ vectors and the $R_{MT}.K_{max}$ parameter were selected in such a way that the total-energy error does not exceed 0.1 mRy. The *local orbitals*[17] for $5s$ and $5p$ states for rare-earth atoms and $2s$ states for the fluorine atoms were added to correct the linearization errors.

The relativistic DFT formalism was employed, but the valence and local orbital states were treated within the scalar approximation, neglecting the spin-orbit (SO) interaction. The spin-orbit interaction was taken into account using the second-variational approach.[18]

III. RESULTS AND DISCUSSION

Within the commonly used approximation, the source of exchange splitting is the interaction between a spin ($\vec{s}$) of photohole created in a core-level and local spin momentum from the partly filled $4f$ shell ($\vec{S}$). The effect is usually described within a framework of the Heisenberg model using the following formula:

$$\Delta H_{ex} = -2J\vec{S}\cdot\vec{s} \tag{1}$$

with the exchange constant J given by a Slater's integral G:

$$J = \frac{1}{2l+1}G^2(4s(5s),4f), \tag{2}$$

where l denotes an orbital momentum of electron from an unfilled shell (l=3 for $4f$ electrons). As a result of this interaction, one observes two lines in the photoemission spectra from the s levels. Thus the exchange splitting of the photoemission lines has been analyzed in relation to the magnetic moment of the partially filled shell.

It is well known that the electronic structure calculations, taking into account the spin polarization of the partially filled d or f shells, can describe the exchange splitting of the valence bands observed experimentally.[19] On the other hand, the spin dependence of the closed-shell electron charge density in magnetic materials is a well-known effect, proven experimentally. Experimental techniques that can measure the nuclear magnetic excitations, e.g., the Mössbauer effect or the nuclear magnetic resonance, provide information about the hyperfine magnetic field (B_{hf}) which acts on the nuclear magnetic moment. There are different sources of the B_{hf}.[20,21] One of them (B_c) originates from the Fermi contact interaction of the nuclear magnetic moment with the electronic magnetization density just inside the nucleus.[22] The dominant contribution to B_c is associated with the magnetization density of the closed-shell s-type electrons.[23,24] The spatial separation of spin-up and spin-down densities of the closed-shell orbitals results from their exchange-correlation interaction with the spin polarized open-shell orbitals.[23,25]

The lack of spin degeneracy of the closed-shell charge density implies the same for single-particle eigenenergies for electrons of closed-shell orbitals. In *all electron* methods of the electronic structure calculations the single electron partial wave functions are calculated with the use of the Kohn-Sham (KS) formalism based on the density-functional theory (DFT). The KS equations solved within the DFT based methods take the form

$$\left(-\frac{\hbar^2}{2m_e}\nabla^2 + v_H(\vec{r}) + v^s_{ext}(\vec{r}) + v^s_{xc}(\vec{r})\right)\phi_i^{KS}(\vec{r},s) = \epsilon_i^{KS}\phi_i^{KS}(\vec{r},s), \tag{3}$$

$$v^s_{xc}(\vec{r}) = \delta E_{xc}[n_\uparrow,n_\downarrow]/\delta n_s(\vec{r}), \tag{4}$$

$$n_s(\vec{r}) = \sum_i^{\epsilon_i<\epsilon_k} |\phi_i^{KS}(\vec{r},s)|^2, \tag{5}$$

where v_H, v_{xc}, and v_{ext} are the Hartree, exchange-correlation, and external ionic potential, respectively. The ϵ_i^{KS} and ϕ_i^{KS} describe the single-electron Kohn-Sham eigenstate. The $E_{xc}[n_\uparrow,n_\downarrow]$ is the functional of exchange correlation energy and $n_s(\vec{r})$ is the electronic spin density. Within *all electron* approaches the n_s stands for the complete spin density of both core and valence electrons. In spin-polarized materials (e.g., with open $3d$ or $4f$ shell elements) the charge density (5) and consequently the exchange correlation potential (4) depend on the spin direction. Within the KS *all electron* approach, both core and valence electrons are treated with the use of Eq. (3) with the same potential function $v_H+v_{ext}+v_{xc}$. The only difference is that the wave functions of the valence and core state electrons fulfill different boundary conditions applied to the partial wave function at the muffin-tin or Wigner-Seitz sphere around an atom. For closed-shell orbitals, the *all electron* spin-dependent v_{xc} potential taken into account in Eq. (3) removes the spin degeneracy of the single-electron eigenvalues, even though the total spin of the close shell remains zero.

To prove the hypothesis that the exchange splitting of the core s level states is to a great extent the ground-state effect, we performed the electronic calculations for Eu, EuF_3, Gd, GdF_3, Tb, TbF_3 and compared the $4s$ and $5s$ level exchange splitting with the experimental data.

The result of our calculations of the exchange spliting are presented in Table I side by side with the experimental values. It appears that the ground-state calculations give results comparable to the photoemission experiment, although the photoemission final-state effects are not included.

In Fig. 1, we show the XPS spectra of the 4s and 5s levels in Eu metal and the EuF_3 MBE grown ultrathin layer. A clear splitting of these levels is visible for both metal and fluoride. The value of exchange splitting in EuF_3 is reduced with respect to Eu metal (in experiment and calculations).

TABLE I. Exchange splitting values for the *s*-type levels in rare-earth elements and compounds; values in brackets come from calculations. The values in square brackets show the spin (S) and orbital (L) momenta of the $4f$ shell, respectively.

ΔE_{ex}(eV)	Gd$\left[\frac{7}{2};0\right]$	GdF$_3\left[\frac{7}{2};0\right]$	Eu$\left[\frac{7}{2};0\right]$	EuF$_3\left[\frac{6}{2};3\right]$	Tb$\left[\frac{6}{2};3\right]$	TbF$_3\left[\frac{6}{2};3\right]$
4s	8.2 (6.2)	8.2 (6.1)	6.8 (5.5)	6.0 (5.1)	7.0 (5.1)	6.2 (5.2)
5s	3.7 (3.3)	3.5 (3.1)	4.0 (3.2)	2.9 (2.7)	3.1 (2.5)	2.9 (2.6)

This can be related to the difference in $4f$ shell occupation (EuF$_3$—$4f^6$; Eu—$4f^7$), which agrees with the number of occupied $4f$ states derived from calculations. Analysis of Table I for Gd, GdF$_3$, Tb, and TbF$_3$ confirms the stable valency of Gd and Tb. The systematic differences between experiment and calculations can be explained due to final-state effects modeled by Eq. (1). The value of ΔE_{ex} is different in Eu metal compared to Gd, which may be related to spatial distribution of $4f$ shell charge density (Eu^{2+} ion is larger than Gd^{3+} and the binding energy of $4f$ level is lower), therefore one can expect weaker $4f$-$4s$ exchange coupling for Eu. For the interaction with the much more extended $5s$ orbitals, the effect is less pronounced. The interesting point is that for EuF$_3$, both $4s$ and $5s$ levels show doublets with splittings that are only slightly smaller than those found in Eu metal.

To describe better the ground state of the $4f$ shell of Eu^{3+} we included in our LSDA+SO calculations the orbital-polarization (OP) term,[26] which approximately accounts for the second Hund's rule. The orbital polarization mainly affects the orbital moment of $4f$ shell of Eu, while the correction of spin moment is negligible. Our calculations, taking into account the orbital polarization interaction within the $4f$ shell, reveal that despite almost exact cancellation of the projected orbital (L) and spin (S) local magnetic moments of Eu in EuF$_3$, the effect of exchange splitting of core $4s$ and $5s$ states of Eu^{3+} persists and its magnitudes are the same as those calculated with the LSDA+SO. Our results correlate very well with the recent investigations of Johannes and Pickett[27] who discussed the magnetic order of Eu^{3+} ions due to spin correlations.

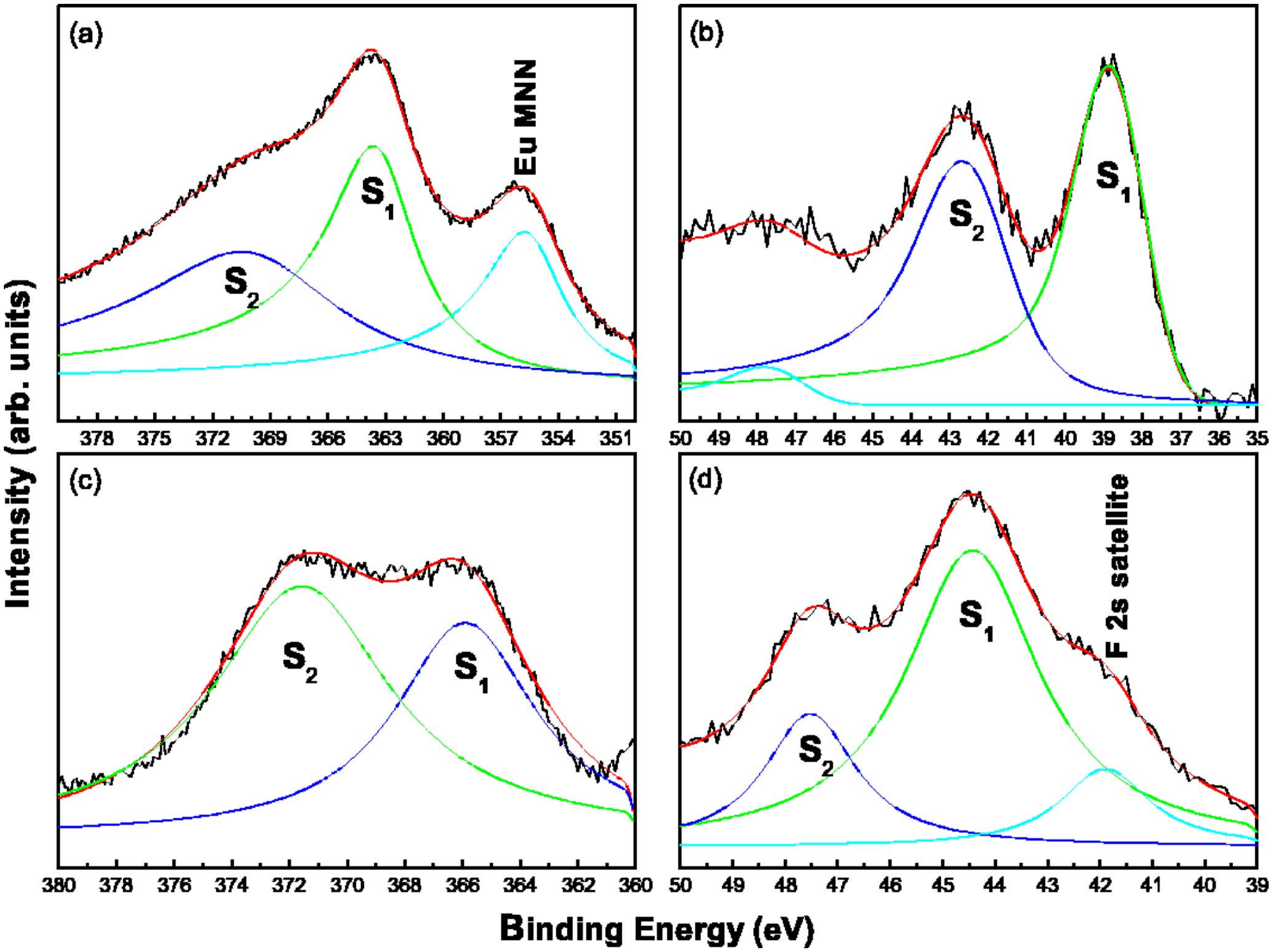

FIG. 1. (Color online) Eu $4s$ and $5s$ level photoemission spectra. Eu metal: (a) 4s, (b) 5s; EuF$_3$ ultrathin layer (MBE): (c) $4s$, (d) $5s$.

IV. CONCLUSIONS

In the present investigations, we showed that in EuF_3, where Eu is trivalent and nonmagnetic (total $4f$ shell angular momentum $J=0$), the core-levels are split due to the exchange interaction of closed-shell orbitals with the spin-polarized charge density of the $4f$ shell. Ground-state ($T=0$ K) electronic structure calculations using the FP-LAPW method give slightly underestimated values of the $5s$ ($4s$) exchange splittings in elemental RE metals (Eu, Gd, Tb) and their trifluorides (EuF_3, GdF_3, TbF_3). The correlation effects, orbital polarization, and spin-orbit coupling taken into account for $4f$ orbitals did not influence the calculated results of splitting. We conclude that the exchange splitting of the closed-shell levels is present in the initial state. It is generated by exchange coupling of these orbitals with the spin-polarized charge density of open-shell orbitals. Our data can be used to complete the diagram of the $5s$ and $4s$ core line splittings in the rare earths and their fluorides[1].

ACKNOWLEDGMENT

We would like to acknowledge financial support from the National Science Foundation (Grant No. DMR-0303563).

---

*Corresponding author. Electronic address: wburian@us.edu.pl

[1] S. Hüfner, *Photoelectron Spectroscopy* (Springer, Berlin, 1995).

[2] J. Szade and M. Neumann, J. Phys.: Condens. Matter **13**, 2717 (2001).

[3] J. Szade, M. Neumann, I. Karla, B. Schneider, F. Fangmeyer, and M. Matteucci, Solid State Commun. **113**, 709 (2000).

[4] E.-J. Cho and S.-J. Oh, Phys. Rev. B **59**, R15613 (1999).

[5] W. Burian, J. Szade, T. O'Keevan, and Z. Celinski, Phys. Status Solidi B **241**, R15 (2003).

[6] J. Szade, W. Burian, Z. Celinski, T. O'Keevan, M. Zangrando, F. Bondino, and E. Magnano, Surf. Sci. **580**, 163 (2005).

[7] P. Blaha, K. Schwarz, G. K. H. Madsen, D. Kvasnicka, and J. Luitz, *WIEN2K, An Augmented Plane Wave + Local Orbitals Program for Calculating Crystal Properties* (Karlheinz Schwarz, Techn. Universitat Wien, Austria, 2001).

[8] K. Takemura and K. Syassen, J. Phys. F: Met. Phys. **15**, 543 (1985).

[9] V. F. Zinchenko *et al.*, J. Alloys Compd. **347**, 1 (2002).

[10] J. J. Hanak and A. H. Daane, Phase Transitions **38**, 127 (1992).

[11] K. Rotereau, P. Daniel, and J. Y. Gesland, J. Phys. Chem. Solids **59**, 969 (1998).

[12] J. S. Olsen, S. Steenstrup, and L. Gerward, Phys. Lett. **109A**, 235 (1985).

[13] M. Piotrowski, H. Ptasiewicz-Bak, and A. Murasik, Phase Transitions **38**, 127 (1992).

[14] J. P. Perdew, K. Burke, and M. Ernzerhof, Phys. Rev. Lett. **77**, 3865 (1996).

[15] V. I. Anisimov, J. Zaanen, and O. K. Andersen, Phys. Rev. B **44**, 943 (1991).

[16] A. B. Shick, A. I. Liechtenstein, and W. E. Pickett, Phys. Rev. B **60**, 10763 (1999).

[17] D. J. Singh, W. E. Pickett, and H. Krakauer, Phys. Rev. B **43**, 11628 (1991).

[18] D. Singh, *Planewaves, Pseudopotentials and the LAPW Method* (Kluwer Academic Publishing, Boston, Dordrecht, London, 1994).

[19] K. Maiti, M. C. Malagoli, A. Dallmeyer, and C. Carbone, Phys. Rev. Lett. **88**, 167205 (2002).

[20] S. Blügel, H. Akai, R. Zeller, and P. H. Dederichs, Phys. Rev. B **35**, 3271 (1987).

[21] M. Battocletti and H. Ebert, Phys. Rev. B **64**, 094417 (2001).

[22] E. Fermi, Z. Phys. **60**, 320 (1930).

[23] J. Deniszczyk and R. Kosimow, J. Phys.: Condens. Matter **10**, 10999 (1998).

[24] J. Deniszczyk, Phys. Status Solidi A **196**, 244 (2003).

[25] A. J. Freeman and R. E. Watson, *Magnetism*, edited by G. T. Rado and H. Suhl (Academic, New York, London, 1965), Vol. IIA, p. 167.

[26] O. Eriksson, M. S. S. Brooks, and B. Johansson, Phys. Rev. B **41**, 7311 (1990).

[27] M. D. Johannes and W. E. Pickett, Phys. Rev. B **72**, 195116 (2005).